Angewandte Chemie
Eine Zeitschrift der Gesellschaft Deutscher Chemiker

Supporting Information

69451 Weinheim, Germany

The Reaction of a High-Valent Nonheme Oxoiron(IV) Intermediate with Hydrogen Peroxide**

Joseph J. Braymer, Kevin P. O'Neill, Jan-Uwe Rohde, and Mi Hee Lim**

anie_201200901_sm_miscellaneous_information.pdf

Table of Contents

Experimental Section

Materials. All reagents were purchased from commercial suppliers and used as received unless stated otherwise. Acetonitrile (CH_3CN), tetrahydrofuran (THF), dichloromethane (CH_2Cl_2), and diethyl ether (Et_2O) were deoxygenated by sparging with N_2 and purified by passage through two packed columns of molecular sieves under an N_2 pressure (MBraun solvent purification system). Preparation and handling of air- and moisture-sensitive materials were carried out in a glovebox under an inert atmosphere of N_2. $Fe(OTf)_2{\cdot}2CH_3CN$ (OTf = trifluoromethanesulfonate) was synthesized by a modified literature method from anhydrous $FeCl_2$ and trimethylsilyl trifluoromethanesulfonate in CH_3CN and recrystallized from CH_3CN/Et_2O.[1,2] The compound $[Fe^{II}(N4Py)(CH_3CN)](OTf)_2$ [**2**$(OTf)_2$, N4Py = *N*,*N*-bis(2-pyridylmethyl)-*N*-[bis(2-pyridyl)methyl]amine] was prepared following the previously reported procedure by addition of $Fe(OTf)_2{\cdot}2CH_3CN$ to a solution of N4Py in THF with a slightly modified work-up.[3,4] After stirring overnight, Et_2O was used to precipitate the orange product, which was recrystallized from CH_3CN/Et_2O. The characterization of the Fe complex by ^{1}H NMR spectroscopy and electrospray ionization mass spectrometry (ESI MS) was in agreement with the previous report of **2**$(ClO_4)_2$ (Figures S2 and S3).[3] The molar extinction coefficients for $[Fe^{II}(N4Py)(CH_3CN)]^{2+}$ (**2**) in CH_3CN were 7.4×10^3 $M^{-1}cm^{-1}$ (λ_{max} = 380 nm) and 5.8×10^3 $M^{-1}cm^{-1}$ (λ_{max} = 454 nm) at 25 °C. $[Fe^{II}(tmc)(OTf)]OTf$ and iodosylbenzene (PhIO) were prepared by literature methods (tmc = 1,4,8,11-tetramethyl-1,4,8,11-tetraazacyclotetradecane).[5,6] Oxidation of the iron(II) complexes (stored in N_2 atmosphere) to the oxoiron(IV) complexes $[Fe^{IV}O(N4Py)]^{2+}$ (**1**) and $[Fe^{IV}O(tmc)(CH_3CN)]^{2+}$ (**7**) was carried out with PhIO as reported.[5,7,8] Diluted aqueous solutions of hydrogen peroxide (H_2O_2) were used for standardizing its 50% (w/w) stock solution (Sigma Aldrich, St Louis, MO, USA) by UV-Vis spectroscopy (λ = 230

nm, ε = 72.4 $M^{-1}cm^{-1}$).[9] Deuterium peroxide (D_2O_2, 30% (w/w) in D_2O) was purchased from Icon Isotopes (Summit, NJ, USA) and standardized using solutions diluted with D_2O in a similar manner to H_2O_2.

UV-Vis Spectroscopy. UV-Vis spectra were recorded on a Hewlett Packard 8453 diode array spectrophotometer with samples maintained at the desired temperature using a cryostat/heater from Unisoku Scientific Instruments (Japan). A typical reaction involved adding 50 μL of a pre-chilled solution of H_2O_2 (50% in H_2O) in CH_3CN to a UV-Vis cuvette (path length, 1.0 cm) containing 2.0 mL of a solution of **1** or **7** in CH_3CN at −20 or 25 °C, respectively. For experiments in a 0.1 cm UV-Vis cuvette, 10 μL of a solution of H_2O_2 in CH_3CN was added to 400 μL of a solution of **1** in CH_3CN. Kinetic experiments for reactions of **1** with an excess of H_2O_2 were monitored at 800 nm to reduce interference from other optical signals [*i.e.*, formation of $[Fe^{III}(N4Py)(OOH)]^{2+}$ (**6**)]. Analysis of pseudo-first-order decay traces of **1** by plotting ln A *versus t* indicated a linear trend for at least three half-lives. For the determination of the observed rate constant (k_{obs}) under pseudo-first-order conditions, data were used from at least three (for **1**) or four (for **7**) experimentally determined half-lives. The fitting of kinetic data and determination of k_{obs} values for **1** and **7** were carried out using the ChemStation software (Agilent Technologies, Santa Clara, CA, USA). Values of k_2' were determined by dividing the second-order rate constant (k_2) by the number (n) of available protons for hydrogen atom transfer (for H_2O_2, n = 2). Kinetic experiments were carried out in triplicate.

ESI(+)MS Measurements. ESI MS measurements were performed with a Micromass LCT time-of-flight mass spectrometer operating in the positive ion mode. Into a septum-sealed

4.0 mL vial, suspended in a cold bath at −20 °C and containing a 1.0 mM solution of **1** in CH_3CN, was injected a solution of 0.5 equiv of H_2O_2 in CH_3CN. Direct introduction of a sample from the reaction mixture into the mass spectrometer *via* a short transfer line was facilitated by applying slight pressure on the headspace of the solution with a syringe. Data were collected at a capillary voltage of 3100 V, a sample cone voltage of 17 V, a desolvation temperature of 100 °C, and a source temperature of 100 °C.

^{1}H NMR Spectroscopy. ^{1}H nuclear magnetic resonance (NMR) spectra were acquired with a Varian 400 MHz instrument at ambient temperature. The reaction of 1.0 mM **1** in CD_3CN with 0.5 equiv of H_2O_2 at −20 °C was monitored by UV-Vis spectroscopy. After no further spectral changes were observed at −20 °C (*ca.* 4 h), the reaction solution was warmed to room temperature (no significant changes were observed in the optical spectrum upon warming). The orange solution was then analyzed by ^{1}H NMR spectroscopy. The NMR spectrum of **1** in CD_3CN prior to the reaction with H_2O_2 was consistent with that previously reported.[8]

EPR Spectroscopy. Electron paramagnetic resonance (EPR) data were collected on a Bruker EMX electron spin resonance spectrometer equipped with an Oxford liquid helium cryostat or a Varian liquid nitrogen cryostat. For the preparation of EPR samples at different reaction time points, the reaction of 1.0 mM **1** in CH_3CN with 0.5 equiv of H_2O_2 at −20 °C was monitored by UV-Vis spectroscopy. At various time points, an aliquot of the reaction mixture was quickly transferred with a chilled Pasteur pipette into an EPR tube pre-cooled to −40 °C and immediately frozen in liquid nitrogen. The EPR sample of $[Fe^{III}(N4Py)(OH)]^{2+}$ (**3**) was prepared from the reaction of **2** (1.0 mM in acetone) with 0.5 equiv of H_2O_2 at room temperature.[10] The

EPR spectra shown in Figure S5 were recorded at 4 K under non-saturating conditions with the instrument operating at 9.37 GHz, a power of 20.5 mW, a modulation frequency of 100 kHz, a modulation amplitude of 10 G, and a resolution in the X direction of 2048 points.

O_2 Detection. Concentrations of O_2 were measured using a borosilicate optical probe with 4.0 mm RedEye^{TM} patches from Ocean Optics (Dunedin, FL, USA; HIOXY coating, calibrated for −20 to 25 °C and 0.0 to 8.0 ppm (mass/mass) of O_2). The experiments were carried out in a threaded 1.0 cm cuvette (Starna Cells, Inc., Atascadero, CA, USA), containing 4.0 mL of solution to minimize headspace and sealed with a septum cap, at a temperature of −20 °C maintained by a cryostat from Unisoku Scientific Instruments. The borosilicate fiber optic probe was positioned with the RedEye oxygen sensing patch within the cuvette, and the entire set-up was then purged with N_2 to remove O_2. The O_2 concentrations were measured upon injection of 100 μL of a thoroughly N_2 purged 0.02 M solution of H_2O_2 in CH_3CN *via* an air-tight syringe into either CH_3CN only, 1.0 mM **1** in CH_3CN, or 1.0 mM **2** in CH_3CN. Concentrations were measured at various time points over 2 h at −20 °C. For experiments with 0.5 equiv of H_2O_2 and 1.0 mM **1** or **2** in CH_3CN, the reaction was continuously monitored by UV-Vis spectroscopy. As a control experiment, the concentration of O_2 in CH_3CN in this set-up was measured over 2 h [0.9 (± 0.1) ppm], verifying minimal O_2 leakage into the cuvette. The measurements for O_2 detection were conducted in triplicate. A calibration curve was created at −20 °C using various concentrations (4.0 – 20 ppm) of O_2 with solutions prepared by dilution of an O_2 saturated CH_3CN solution (8.1 mM O_2 in CH_3CN at 25 °C).[11] The theoretical yield of 20.3 ppm of O_2 for the reaction of **1** with H_2O_2 (based on a 2:1 stoichiometry between **1** and the produced O_2) was found to correspond to a sensor reading of 13.7 (±0.4) ppm.

References

[1] J. Arnold, C. G. Hoffman, D. Y. Dawson, F. J. Hollander, *Organometallics* **1993**, *12*, 3645.

[2] K. S. Hagen, *Inorg. Chem.* **2000**, *39*, 5867.

[3] M. Lubben, A. Meetsma, E. C. Wilkinson, B. Feringa, L. Que, Jr., *Angew. Chem.* **1995**, *107*, 1610; *Angew. Chem. Int. Ed.* **1995**, *34*, 1512.

[4] J.-U. Rohde, S. Torelli, X. Shan, M. H. Lim, E. J. Klinker, J. Kaizer, K. Chen, W. Nam, L. Que, Jr., *J. Am. Chem. Soc.* **2004**, *126*, 16750.

[5] J.-U. Rohde, J.-H. In, M. H. Lim, W. W. Brennessel, M. R. Bukowski, A. Stubna, E. Münck, W. Nam, L. Que, Jr., *Science* **2003**, *299*, 1037.

[6] H. Saltzman, J. G. Sharefkin, *Org. Synth.* **1963**, *43*, 60.

[7] J. Kaizer, E. J. Klinker, N. Y. Oh, J.-U. Rohde, W. J. Song, A. Stubna, J. Kim, E. Münck, W. Nam, L. Que, Jr., *J. Am. Chem. Soc.* **2004**, *126*, 472.

[8] E. J. Klinker, J. Kaizer, W. W. Brennessel, N. L. Woodrum, C. J. Cramer, L. Que, Jr., *Angew. Chem.* **2005**, *117*, 3756; *Angew. Chem. Int. Ed.* **2005**, *44*, 3690.

[9] P. George, *Biochem. J.* **1953**, *54*, 267.

[10] G. Roelfes, M. Lubben, K. Chen, R. Y. N. Ho, A. Meetsma, S. Genseberger, R. M. Hermant, R. Hage, S. K. Mandal, V. G. Young, Jr., Y. Zang, H. Kooijman, A. L. Spek, L. Que, Jr., B. L. Feringa, *Inorg. Chem.* **1999**, *38*, 1929.

[11] S. V. Kryatov, E. V. Rybak-Akimova, S. Schindler, *Chem. Rev.* **2005**, *105*, 2175.

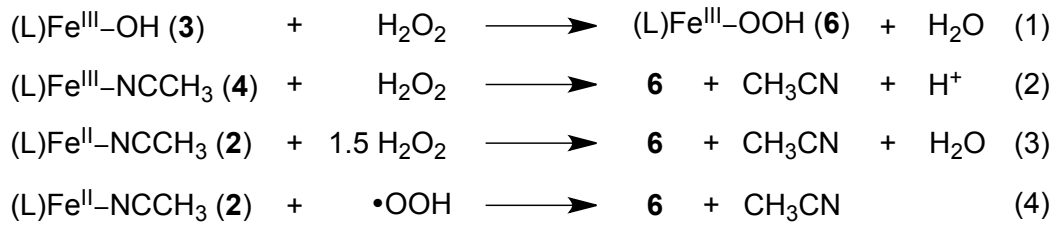

Scheme S1. Possible pathways to generate **6** when an excess of H_2O_2 is present in the reaction with **1** (Scheme 1).

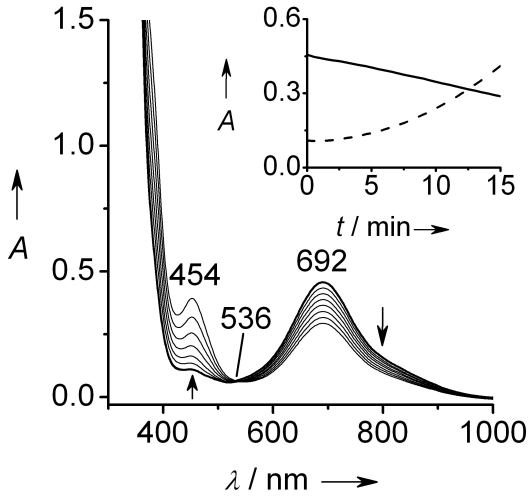

Figure S1. UV-Vis spectra of the first 15 min of the reaction of 1.0 mM **1** in CH_3CN (bold line) with 0.5 equiv of H_2O_2 at −20 °C (path length, 1.0 cm; *cf.* Figure 1). Inset: Time courses of the decay of **1** (λ = 692 nm, solid line) and the formation of **2** (λ = 454 nm, dashed line).

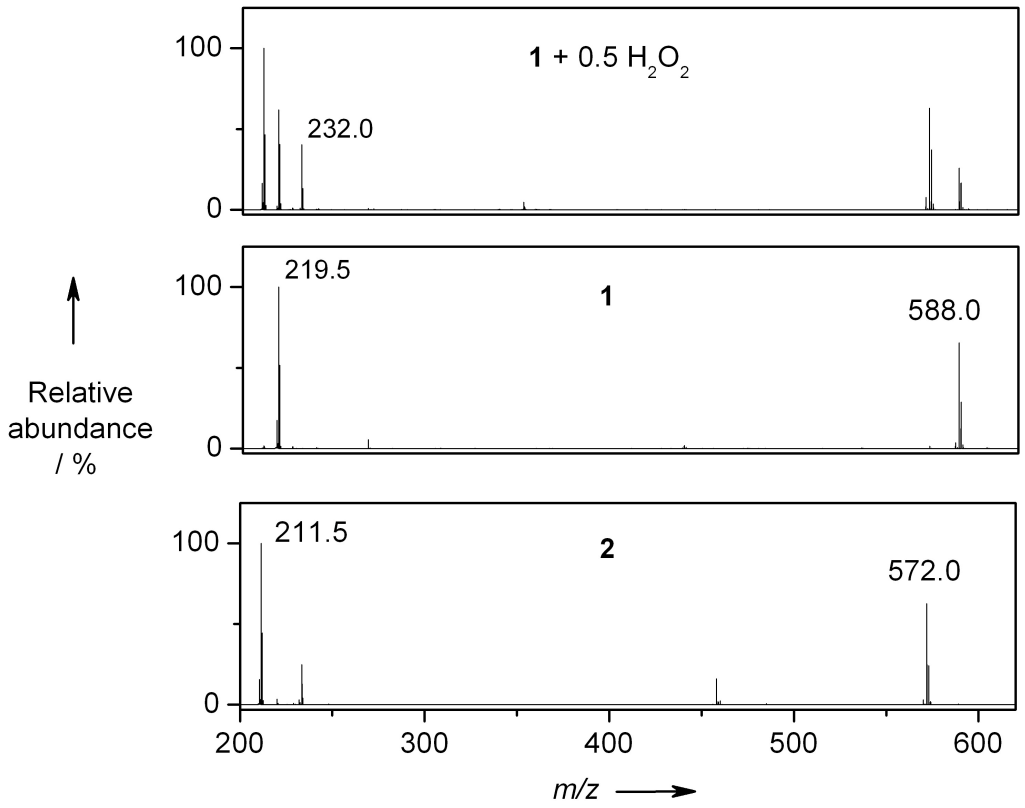

Species	Observed (*m/z*)	Calculated (*m/z*)
$[Fe^{II}(N4Py)]^{2+}$	211.5	211.6
$\{[Fe^{II}(N4Py)] + CH_3CN\}^{2+}$	232.0	232.1
$\{[Fe^{II}(N4Py)] + OTf\}^{+}$	572.0	572.1
$[Fe^{IV}O(N4Py)]^{2+}$	219.5	219.5
$\{[Fe^{IV}O(N4Py)] + OTf\}^{+}$	588.0	588.1

Figure S2. ESI(+) mass spectra of **1**, **2**, and the products of the reaction of 1.0 mM **1** in CH_3CN with 0.5 equiv of H_2O_2 at −20 °C (top) and summary of the observed and calculated *m/z* values (bottom).

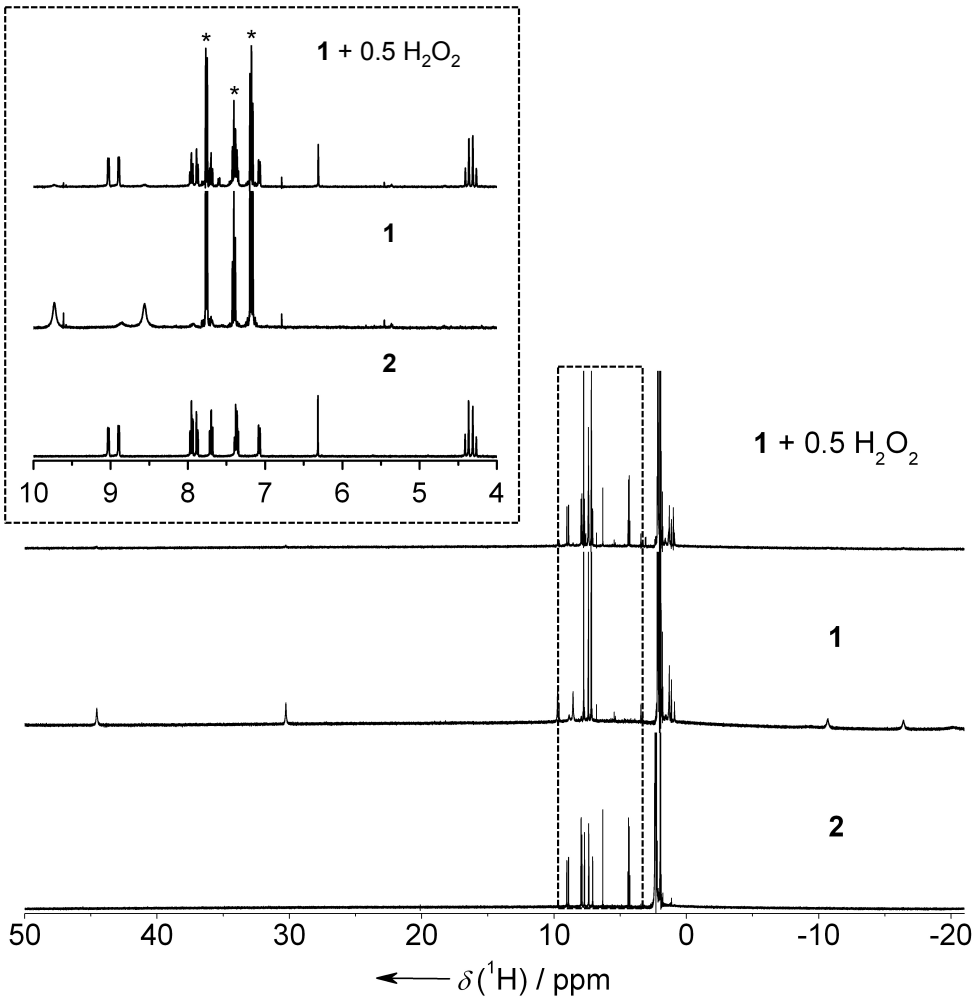

Figure S3. ^{1}H NMR spectra of **1**, **2**, and the products of the reaction of 1.0 mM **1** with 0.5 equiv of H_2O_2 (−20 °C) in CD_3CN. Spectra were recorded at room temperature (400 MHz). Inset: Expanded view of the region from 4 to 10 ppm. The asterisks (*) indicate the ^{1}H NMR signals of iodobenzene.

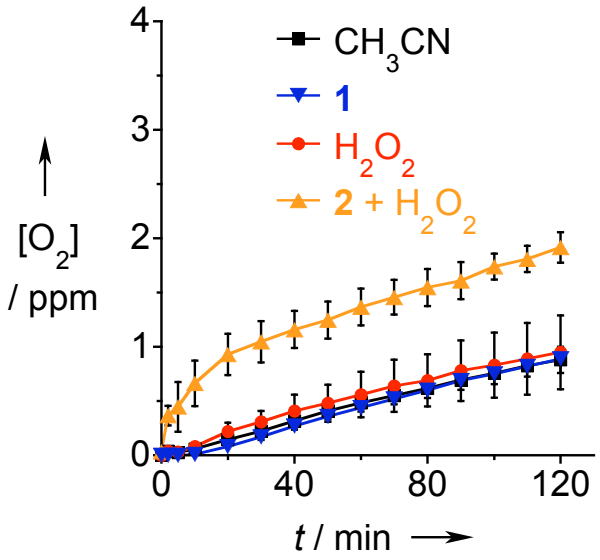

Figure S4. Control experiments for the detection of O_2 over time in CH_3CN (black squares), in a 1.0 mM solution of **1** in CH_3CN (blue inverted triangles), and upon addition of 100 μL of a 0.02 M solution of H_2O_2 (in CH_3CN) to CH_3CN (red circles) and to 1.0 mM **2** in CH_3CN (orange triangles). The measurements were conducted at –20 °C and in triplicate.

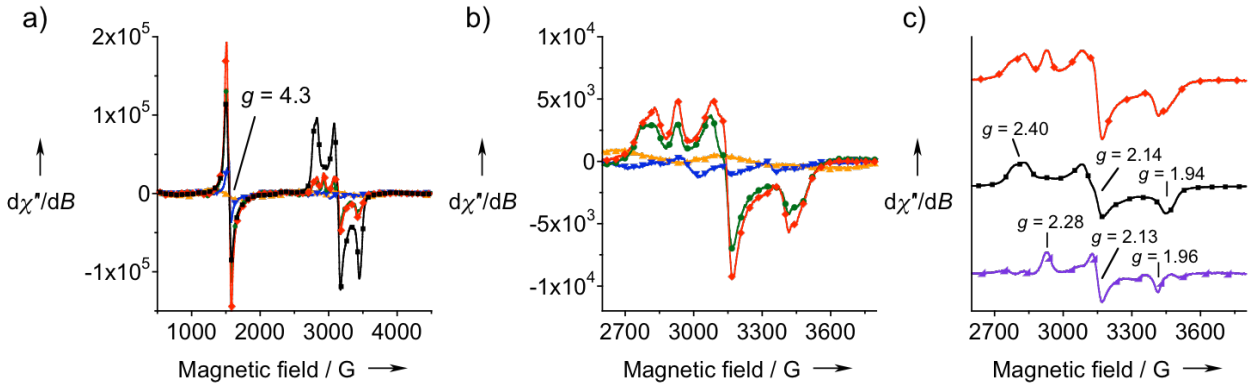

Figure S5. EPR spectra of the reaction of 1.0 mM **1** in CH_3CN at −20 °C with 0.5 equiv of H_2O_2. a) EPR spectra (recorded at 4 K) of frozen samples of 1.0 mM solutions of **1** (blue inverted triangles) and **2** (orange triangles) in CH_3CN and of samples of the reaction of 1.0 mM **1** with 0.5 equiv of H_2O_2 (in CH_3CN at −20 °C) frozen at *ca.* 22 min (green circles) and at nearly complete decay of **1** (*ca.* 100 min, red diamonds). Also shown is the EPR spectrum of independently generated **3** (1.0 mM in acetone, black squares). EPR signals shown in a) were magnified by a factor of five except for that of **3**. b) Expanded view of the region from 2600 to 3800 G. c) Difference EPR spectrum (purple right-angled triangles) generated by subtraction of the spectrum of **3** (reduced by a factor of 25, black squares) from that of the reaction mixture (*ca.* 100 min, red diamonds).

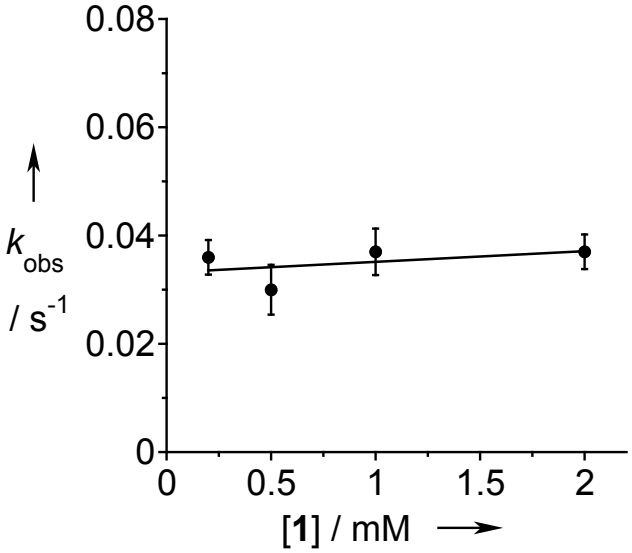

Figure S6. Plot of the pseudo-first-order rate constant (k_{obs}) *versus* [**1**] (0.2 – 2.0 mM) for the reaction of **1** with 50 mM H_2O_2 in CH_3CN at −20 °C.

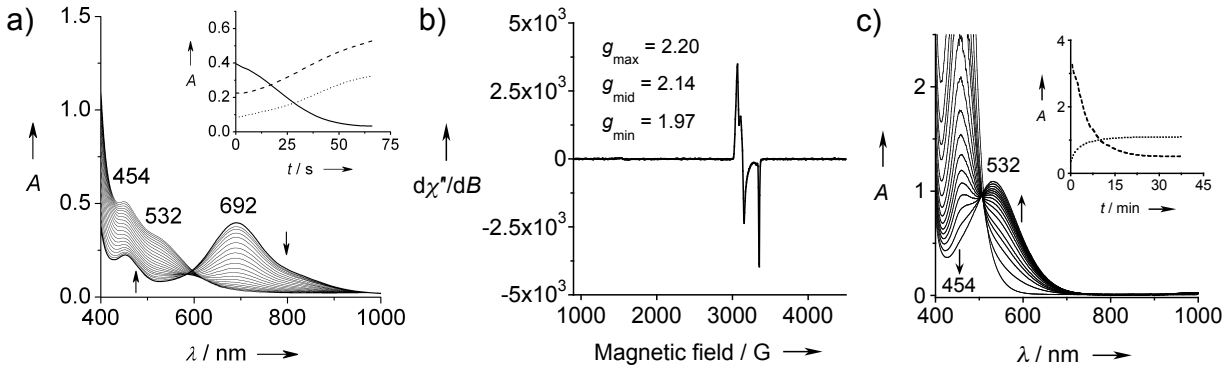

Figure S7. Evidence for the formation of **6** in the reaction of **1** with an excess of H_2O_2. a) UV-Vis spectra of the first 1 min of the reaction of 1.0 mM **1** in CH_3CN (bold line) with 50 equiv of H_2O_2 at −20 °C (path length, 1.0 cm). Inset: Time courses of the decay of **1** (λ = 692 nm, solid line), formation of **2** (λ = 454 nm, dashed line), and formation of **6** (λ = 532 nm, dotted line). b) EPR spectrum of a sample obtained upon consumption of **1** in the reaction of 1.0 mM **1** with 20 equiv of H_2O_2 (in CH_3CN at −20 °C). This spectrum was recorded at 77 K under non-saturating conditions with the instrument operating at 9.26 GHz, a power of 20.5 mW, a modulation frequency of 100 kHz, a modulation amplitude of 10 G, and a resolution in the X direction of 1024 points. c) UV-Vis spectra of the formation of **6** (λ_{max} = 532 nm) upon the addition of 700 equiv of H_2O_2 to 1.0 mM **2** in CH_3CN at −20 °C (path length, 1.0 cm). Inset: Time courses of the decay of **2** (λ = 454 nm, dashed line) and formation of **6** (λ = 532 nm, dotted line).

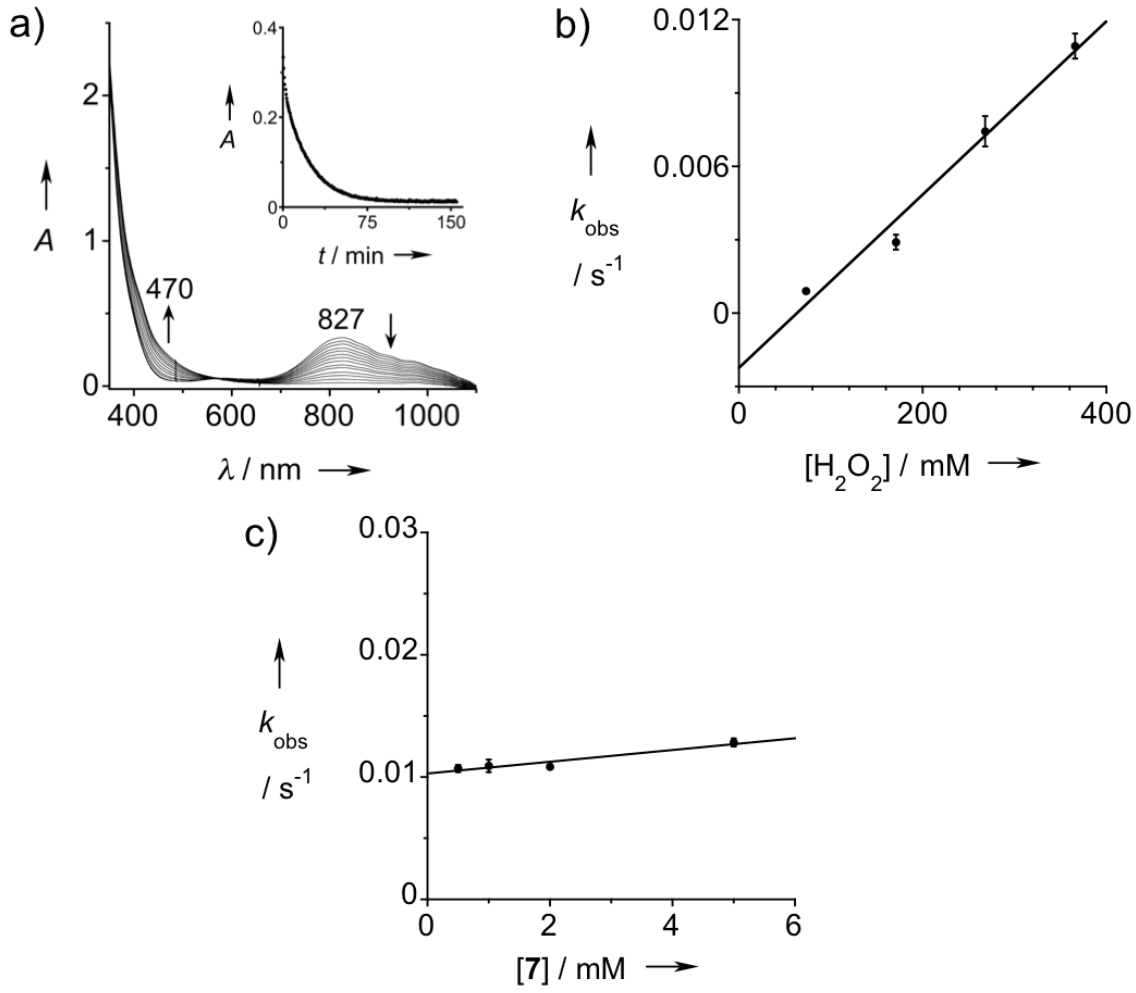

Figure S8. Kinetic results for the reaction of **7** with H_2O_2 in CH_3CN at 25 °C. a) UV-Vis spectra of the reaction of 1.0 mM **7** in CH_3CN (λ_{max} = 827 nm) with 75 equiv of H_2O_2 (path length, 1.0 cm). Inset: Time course of the reaction (λ = 827 nm). b) Plot of k_{obs} *versus* [H_2O_2] (73 – 366 mM) for the reaction of 1.0 mM **7** with H_2O_2. c) Plot of k_{obs} *versus* [**7**] (0.5 – 5.0 mM) for the reaction of **7** with 366 mM H_2O_2.